Properties of Soy Protein Isolate/Poly(vinyl alcohol) Blend "Green" Films: Compatibility, Mechanical Properties, and Thermal Stability

Jun-Feng Su,[1,2] Zhen Huang,[2] Chuan-Min Yang,[2] Xiao-Yan Yuan[1]

[1]*School of Material Science and Engineering, Tianjin University, Tianjin 300072, China*
[2]*Department of Packaging Engineering, Tianjin University of Commerce, Tianjin 300134, China*

Received 27 April 2008; accepted 5 July 2008
DOI 10.1002/app.28979
Published online 17 September 2008 in Wiley InterScience (www.interscience.wiley.com).

ABSTRACT: Blend films from nature soy protein isolates (SPI) and synthetical poly(vinyl alcohol) (PVA) compatibilized by glycerol were successfully fabricated by a solution-casting method in this study. Properties of compatibility, mechanical properties, and thermal stability of SPI/PVA films were investigated based on the effect of the PVA concentration. XRD tests confirm that the SPI/PVA films were partially crystalline materials with peaks of $2\theta = 20^\circ$. And, the addition of glycerol will insert the crystalline structure and destroy the blend microstructure of SPI/PVA. Differential scanning calorimetry (DSC) tests show that SPI/PVA blend polymers have a single glass transition temperature (T_g) between 80 and 115.0°C, which indicate that SPI and PVA have good compatibility. The tension tests show that SPI/PVA films exhibit both higher tensile strength (σ_b) and percentage elongation at break point (P.E.B.). Thermogravimetric analysis (TGA) and water solubility tests show that SPI/PVA blend polymer has more stable stability than pure SPI. All the results reflect that SPI/PVA/glycerol blend film provides a convenient and promising way to prepare soy protein plastics for practical application. © 2008 Wiley Periodicals, Inc. J Appl Polym Sci 110: 3706–3716, 2008

Key words: soy protein isolate; poly(vinyl alcohol); compatibility; mechanical properties; thermal stability

INTRODUCTION

In recent years, the development of environment-friendly and biodegradable materials based on nature polymers, especially from agriculture products including cellulose, starch, and protein materials, have received increasing attention in an attempt to substitute existing petroleum-based polymers.[1] Among these various natural materials, soy protein-based plastics have been extensively studied as a potential replacement owing to their low cost, easy availability, and complete biodegradability.[2] Especially, soy protein isolate (SPI) contains more protein than any other soy protein products, which leads it to hold a higher film forming ability for packaging films,[3] edible films,[4] and skin repair films.[5] Moreover, these SPI functional films have properties of good biodegradable performance, high barrier properties against oxygen, and effective resistance of oil movement in low relative humidities.[6–8]

Besides the above-mentioned good characteristics of SPI films, there is still an inherent problem limiting them in usages, i.e., lower mechanical properties.[9] Pure SPI films cannot be used directly because of their brittle fracture. To improve the mechanical properties, various researches have been carried out to modify SPI materials through physical,[2,10–12] enzymatic,[13] chemical, and physicochemical methods.[14–17] A survey of relevant literature reveals that the mechanism of all these methods is to increase the crosslinkage of protein molecules. SPI possesses many side reactive groups such as —NH_2, —OH, and —SH, which are easy to occur crosslinking reactions. Fundamentally, all these methods can be classified into two approaches. The first approach consists of modifying the primacy structure of SPI by graft reaction[18] or monomer reaction.[19] The second approach is to modify the protein structure in the film-forming solutions through denaturation or reactive blending with other plasticizers or biodegradable polymers. Plasticizers is extensively employed in SPI materials, which can increase the flexibility and elasticity of plastics because of their ability to reduce internal hydrogen bonding between polymer chains while increasing molecular spacing. For example, glycerol, as a plasticizer, has been widely used to improve the toughness and to make the SPI resin more flexible.[10] Unsatisfactorily,

Correspondence to: J.-F. Su (sujunfeng2000@yahoo.com.cn).

Contract grant sponsor: National Key Technology R and D Program of China; contract grant number: 2006BAD05A05.

glycerol is bound to the protein molecules via weak hydrogen bonds and always leaches out over time, greatly affecting the resin's mechanical properties.[20] One way to overcome this problem is to use an internal plasticizer that can chemically bound to protein molecules via strong covalent bonds, and thus prevent the glycerol from leaching out. Normally, after the formation of chemical bond in protein molecules, the protein has been denatured. Denaturation is normally defined as the modification of the secondary, tertiary, and quaternary structure of protein macromolecules including methods of exposure to acid, alkali, detergent, heat, or radiation. However, such denaturation methods without other long-molecular addition still do not show, in most cases, satisfactory physicochemical and mechanical properties for industrial applications.[21] Therefore, SPI blended with biodegradable polymers will be a promising method for modifying SPI structure and have already received most attention to increase the foundational properties of SPI films.[1,21,22] Literature shows that both of synthetic and natural biodegradable polymers have been investigated as secondary components.[21,22] Recently, we have reported that the mechanical properties of SPI films can be improved by blending with poly(vinyl alcohol) (PVA).[23] Moreover, we have confirmed that the SPI/PVA films are "green" materials with good biodegradability in our previous study.[23] As PVA is the largest synthetic water-soluble polymer produced in the world, it can be blended with other natural polymers to form biodegradable composites. Moreover, these PVA/natural polymers blends have promising industrial applications in many fields because of their biodegradability, biocompatibility, chemical resistance, and excellent physical properties.

Based on the above-mentioned background and the drive of the fundamental research and industrial application, the objective of this work was to fabricate solution-casting films from SPI and long-chain molecules of PVA and to investigate the compatibility, mechanical properties, and thermal stability of the blends. To increase the flexibility and modify the interfacial adhesion of the blend, glycerol was added into blend film in this study.[11] The compatibility of SPI/PVA blends was tested to understand the blend structure. The effect of PVA contents in SPI/PVA films on the mechanical and thermal properties of two series of blends with/without glycerol was comparatively investigated. Mechanical properties were studied through tension tests by comparing the parameters of tensile strength (σ_b), percentage elongation at break point (P.E.B.), and Young's modules (E). Through this blend method, it was expected that not only long-chain PVA molecules might increase the mechanical properties and thermal stability of SPI films, but also the little molecules of glycerol would be helpful in enhancing the toughness of SPI films.

EXPERIMENTAL

Materials

SPI powder (Type C©) with moisture content less than 5.0% prepared at acid precipitation and containing more than 90% protein was provided by Harbin High-technology soy protein (Harbin, China). PVA with weight–average molecular weight (M_w) of 1.0×10^5 and minimum degree of hydrolysis of 87% was purchased from SINPEC Shanghai Petrochemical. SPI and PVA were vacuum-dried at 50°C for 24 h before use. Analytical grades of glycerol (1,2,3-propane-triol) of 95% purity and sodium hydroxide (NaOH) were acquired from Tianjin Chemical without further treatment. Analytical grade of NaOH pellets was applied to prepare a 2.0 mol/L solution at room temperature in the laboratory.

Preparation of SPI/PVA blend films

Fabrication of SPI/PVA films was based on a solution casting and evaporation process. The mixture solution was prepared as previously described.[23] Briefly, a typical sample was prepared according to the following steps. First, SPI water solution was prepared by adding 5 g of SPI powder to 100 g of deionized water, in which pH value was adjusted to 10.0×2.0 mol/L NaOH solution with continuous 200 rpm stirring rate at 80°C for 60 min. The pH value of this solution was monitored using an electronic pH-meter (660 Type, Lengpu, Shanghai). The reason of turning pH to 10.0 has been well known to give a maximum protein unfolding and rearrangement station.[24] This pH value will also bring high lysino-alanine linkage formation and high hydrolysis of asparagines and glutamine primary residues. Second, 10% (wt %) PVA water solution was stir-heated in a water bath maintained at 90°C for 60 min. Then, a mixture including the prepared SPI solution, various weight ratios of 10% PVA water solution, and glycerol was formed as the film resin. The film resin was again adjusted to pH = 10.0 with the 2.0 mol/L NaOH solution at 80°C and stirred-heated for 30 min. At last, the mixed resin, after vacuum defoamation process, was poured on a Teflon-coated metal sheet to fabricate SPI films. Uniform film thickness could be achieved by casting the same amount of film-forming solution on each plate with the same area. The Teflon-coated metal sheet was dried in an oven at 50°C for 6 h and then cooled down to room temperature for 24 h. After drying, films were peeled from the sheet perfectly. Then, the films were kept at room temperature in a conditioning

desiccator of 43% relative humidity (RH) (conditioned by $CaCO_3$ saturated solution) for 3 days before being tested. Specimens were cut into demanded sizes for investigating of morphologies, mechanical properties, and thermal properties.

By the control of the weight ratios of SPI/PVA, such as 100/0, 95/5, 90/10, 85/15, 80/20, 75/25, 70/30, and 60/40, a series of SPI/PVA films were coded as P-0, P-5, P-10, P-15, P-20, P-25, P-30, and P-40, respectively. Another series of SPI/PVA films was prepared using earlier method mixed with glycerol. These resulting films were coded as P-PVA-*n*, where *n* is the weight percent of glycerol based on SPI. For example, P-10-2 means the weight ratio of SPI and PVA was 90/10 in the blend films, i.e., the glycerol percent based on SPI was 2.0 wt %.

Characterizations

Surface morphologies

The surface morphologies of samples were characterized using a scanning electron microscope (SEM, XL30 PHILIPS) at an acceleration of 5 kV. The samples were adhered by double-side electrically conductive carbon tape and then coated with thin gold layers about 200 Å before observation.

XRD analysis

Pure PVA and pure SPI in powder form and SPI/PVA blend with/without glycerol in film form were used to obtain their X-ray diffraction patterns by using a powder diffractometer (Rigaku D/max 2500v/pc, Japan). The specimens were scanned from 5° to 60° (2θ) at 2°/min applying the Cu-Kα X-ray radiation of 0.1542 nm. The patterns were analyzed to estimate the percentage of the crystallinity of the specimens.

Differential scanning calorimetry analysis

DSC was applied to analyze the glass transition temperatures (T_g) for the blend films. These tests were performed using a DSC TA2010 controlled by a TA5000 system (TA Instruments, New Castle, DE). The testing temperature is in the range of 0–250°C. The samples (10 mg) were placed in hermetically sealed aluminum TA pans and heated at 5°C/min. The T_g corresponded to the temperature where a baseline inflection occurred, and the melting temperature was determined as the peak temperature of the endothermic event of the DSC curves.

FTIR analysis

These film samples were dried in vacuum at room temperature for 24 h and cut into small pieces to be pelletized with KBr before the measurement of Fourier transform infrared spectra (FTIR). FTIR spectra were obtained on the NICOLET Magna 750 spectrometer with DTGS detector and OMNIC 3.2 software using 128 scans at a resolution of 4 cm^{-1} in a range of wavenumber from 4000 to 400 cm^{-1}.

Mechanical properties

All film specimens were conditioned for 2 days in an environmental chamber at 25°C with 50% RH before testing. Five samples (25 mm × 100 mm) for each film were tested. Thickness of samples was measured with a micrometer having a sensitivity of 1 μm. Tensile strength (σ_b) and percentage of elongation at break point (P.E.B.) were determined by an AG-IS model analyzer (Shimadzu, Japan) according to ASTM D882-97 (ASTM, 2000b) procedure at the strain rate of 5 mm/min. Young's modules was calculated from the tensile stress–strain plots by the computer software. The values presented here are average of five samples.

TGA analysis

The thermal stability characterization was performed on a Dupont SDT-2960 TGA analyzer and in the following conditions: sample weight 50 mg, reference material α-Al_2O_3, heating rate of 5°C/min with a flow of 40 mL/min nitrogen. And, the testing temperature is in the range of 0 to 800°C.

Water solubility

A method modified from Martelli et al.[25] was used to determine the solubility of films in water. Films were cut into 50 mm × 50 mm pieces and dried at 70°C and 96 kPa in a vacuum oven for 24 h. After drying, films were weighed to the nearest 0.01 g for the determination of the initial dry weights of films. Films were individually placed into in a 250 mL beaker with 200 mL of distilled water. The beaker was capped and placed in a shaking water bath at 25°C ± 0.1°C for a period of time. By comparing and recording the shapes of films in water using a camera, we can distinguish the preferable sample owing higher thermal stability. The solubility of films was recorded at other temperatures of 20, 40, 60, 80, and 100°C by using this method, respectively. During the dissolution process, film pieces in water can be then filtrated out by pledget at a point of time and then dried at 70°C and 96 kPa in a vacuum oven for 24 h to determine the final dry weight of films. Three replicates of each film were done. Percent total soluble matter was calculated from the

initial and final dry weights of films and reported on dry weight basis following the eq. (1),

$$D = \frac{W_0 - W_1}{W_0} \times 100\% \quad (1)$$

where W_0 and W_1 are the weights of the films before and after being dissolved.

RESULTS AND DISCUSSION

Surface morphologies of films

Figure 1 shows general photographs of SPI/PVA rolling films. Each sample has the size about of 50 cm × 50 cm, which is large enough for mechanical properties and thermal stability characterization. Seven films, fabricated with the increasing weight ratio of PVA in films [from left to right in Fig. 1(a)], are in rolling state. The surface of films is very smooth and brightness as shown in Figure 1(b). In Figure 1(c), the print words in a paper under a film can be seen distinctly in bright light with good transparence. Figure 2(a–d) typically shows the SEM morphologies of P-0, P-10, P-10-1, and P-10-3, respectively. Obviously, these films can be fabricated smoothly on Teflon-coated metal sheet without cracks and microholes. With the addition of glycerol in SPI/PVA, the surfaces have some rimples, which might owe to the toughness effect of little molecules.

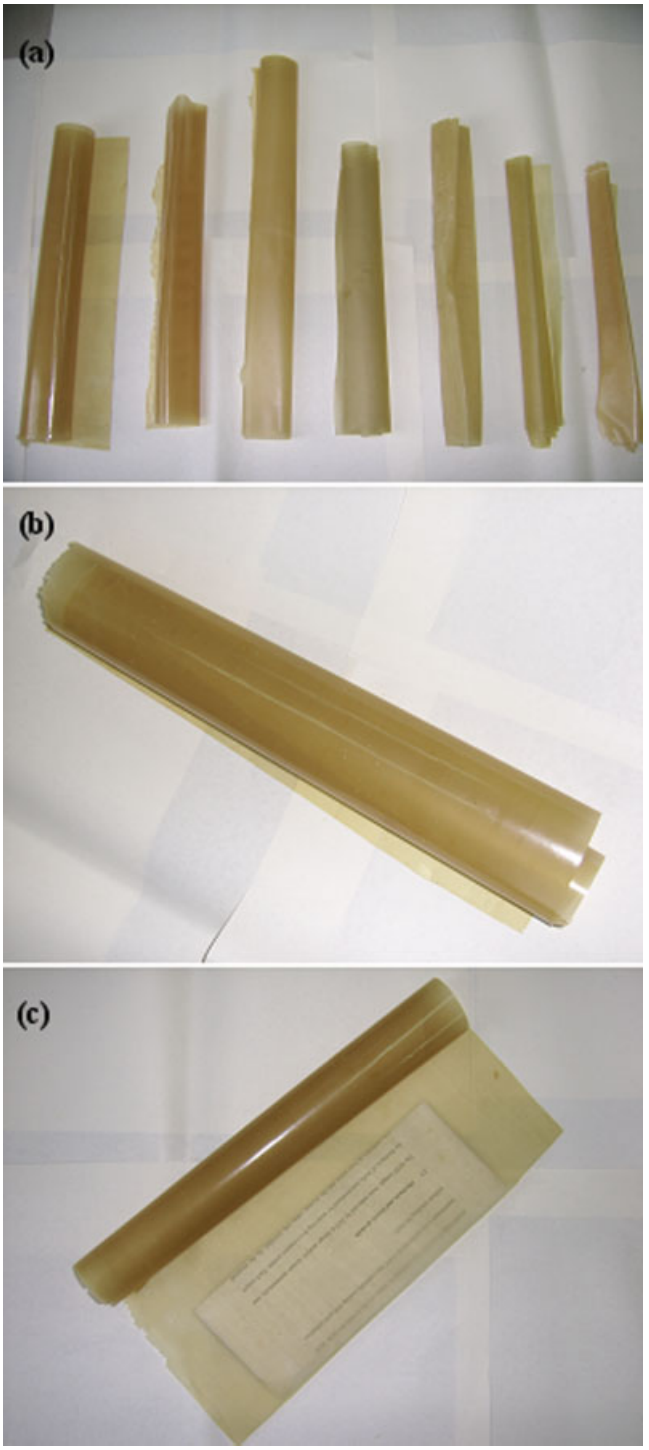

Figure 1 Photographs of SPI/PVA rolling films, (a) the films express as the total difference in color depending on content of PVA, (b) films have good toughness smooth and brightness surfaces and are softer enough to rolled into tubbiness, (c) the print words in a paper under a film can be seen distinctly in bright light. [Color figure can be viewed in the online issue, which is available at www.interscience.wiley.com.]

Compatibility of SPI/PVA blends

Blend solution of SPI and PVA with various weight ratios appeared to be homogeneous at a macroscopic level. However, Bourriot et al.[26] have reported that a mixed biopolymer system is thermodynamically unstable, and a phase separation may not be observed on the experimental time scale because of kinetic energy barriers associated with the restricted movement of biomacromolecules through biopolymer networks. If different polymers were incompatible, they would repel each other following with thermodynamic phase separation. Also, Cho et al.[27] reported films formed from natural polymeric ingredients tended to be brittle, and plasticizers were normally added to a polymeric matrix before drying to overcome the brittleness of films. Therefore, it is essential to understand the compatibility between SPI and PVA in this study. Usually, XRD tests are applied to investigate the crystal structures and crystal degrees for understanding the compatibility of blends. For synthetic polymer of PVA, researches have shown that composites of PVA-based/natural polymers (including starch, cellulose, chitin, chitosan, wheat protein, egg protein, lignin, sodium alginate, etc.) have good biodegradability and

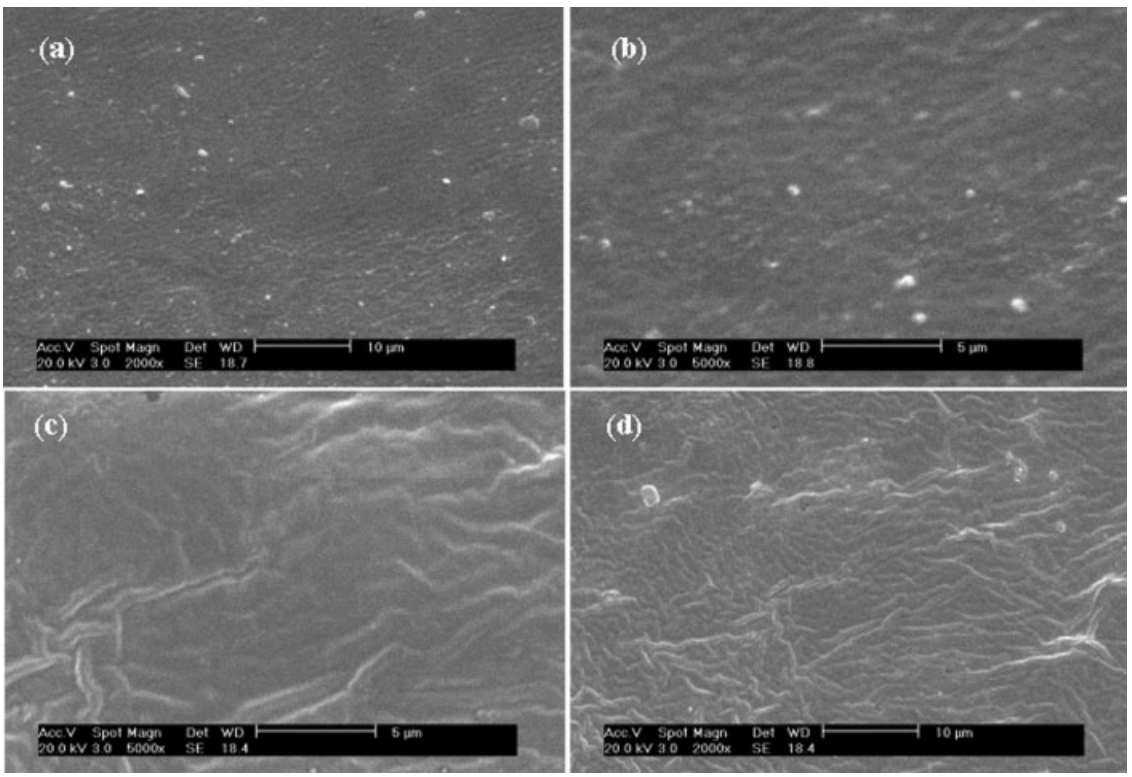

Figure 2 SEM morphologies of film samples, (a) P-0, (b) P-10, (c) P-10-1, and (d) P-10-3.

biocompatibility.[15] For example, Chiellini et al.[28] have found that the diffraction pattern of PVA dominated in the composite and the crystalline of starch nanocrystals by the strong interactions between PVA and starch molecules.

Figure 3 shows the typical X-ray patterns of the pure PVA powder, pure SPI powder, P-10, P-20, and P-20-2 according to the curves of a, b, c, d, and e. First of all, PVA has a strong characteristic peak at $2\theta = 20^\circ$, which is agreeing with the results obtained by Kaczmarek and Podgórski[29] working with pure PVA films and our previous work.[23] And, pure SPI gives a strong characteristic peak at 2θ values of around 22°. With the weight ratio of 90/10 for SPI and PVA, P-10 has two strong peaks at 2θ value of about 19° and 22°. However, the peaks intensity decreased a lot when compared with those of pure PVA and SPI. This indicates that the crystalline structure of either PVA or SPI has collapsed after blended with each other. Yakimets et al.[30] have also found similar results that the XRD curves have multipeaks in studying the crystallinity of gelatin/PVA films. Also, Xiao and Gao[31] have reported that PVA has a flexible structure, which favor close molecular packing and crystallization. With the addition of glycerol in blend films, the XRD peaks are gentler by comparing the XRD patterns of P-20 and P-20-2, which indicate that the presence of glycerol reduces the crystallinity of PVA/SPI blend. Through all these results, it is concluded that the blend films from SPI and PVA would be partially crystalline materials, and the addition of glycerol can insert the crystalline structure and regulate the microstructure of SPI/PVA blends.

To understand the effect of glycerol on the blend crystalline structure better, the XRD peaks for samples of P-30-0, P-30-1, P-30-2, P-30-3, and P-30-4 are shown in Figure 4. The reason for only selecting sample of P-30 with higher weight content of PVA is that we can clearly investigate the changes of glycerol addition on crystalline degrees for SPI/PVA blends through strong XRD peak intensity. According to the above discussion, we know that the peaks of XRD for SPI/PVA blends are in the range of 10°–30°. Therefore, to explain the profound things in a simple way, only XRD curves from 10° to 30° are shown to contrast the peaks intensity. Comparing the five XRD patterns, we can obviously achieve the conclusion that the glycerol has destroyed the crystalline structure. Concretely, samples of P-30-0, P-30-1, and P-30-2 have characteristic peak at 2θ values of around 22°. Especially, the P-30-0 has a higher crystalline degree without compatibility of glycerol. With the increasing of glycerol addition from 1 to 2%, the XRD characteristic peak values at 2θ for P-30-1 and P-30-2 decreased distinctly. Meanwhile, with the increasing of glycerol, the XRD characteristic peak for P-30-3 and P-30-4 shift to 20°–21°, and the XRD peaks are gentler. All these results confirm that the glycerol inserts into the macromolecular

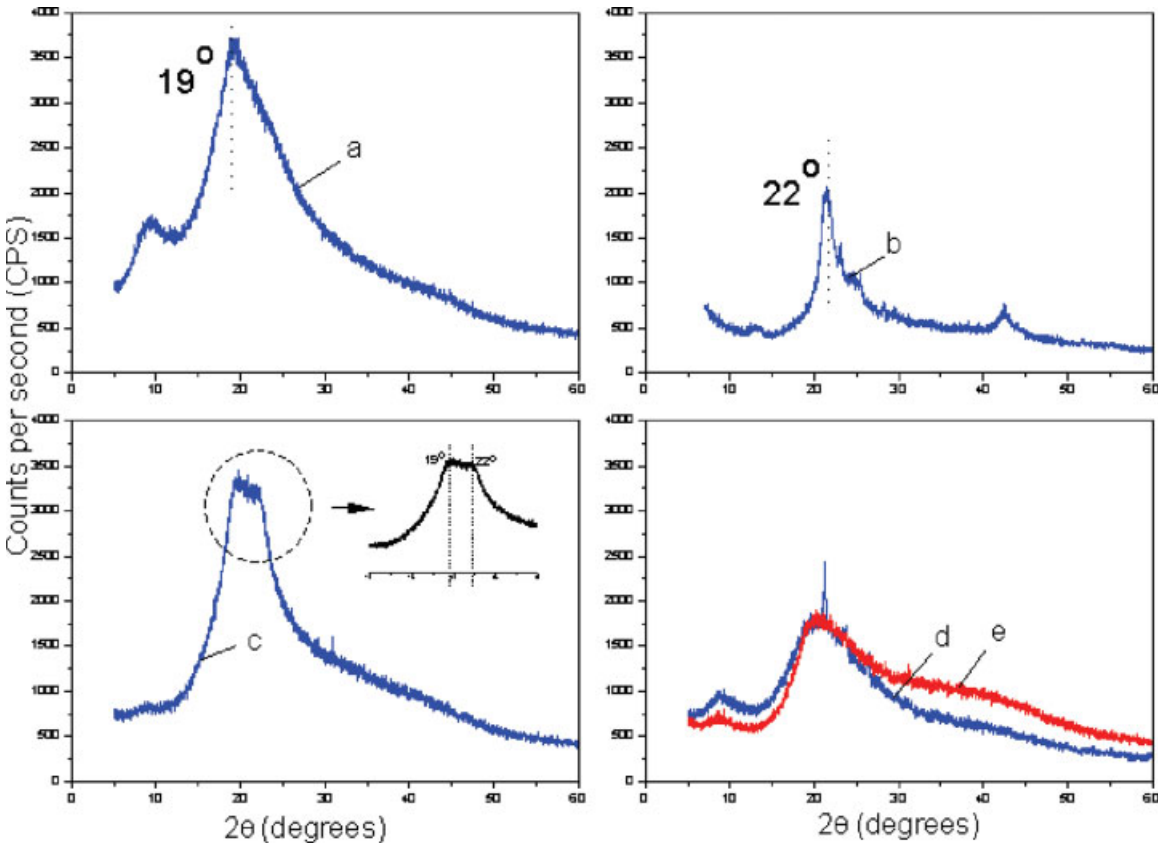

Figure 3 X-ray patterns of the pure PVA powder, pure SPI powder, P-10, P-20, and P-20-2 according the curves of a, b, c, d, and e. [Color figure can be viewed in the online issue, which is available at www.interscience.wiley.com.]

blending structure and destroy the crystalline of blends. Moreover, the addition of glycerol in SPI/PVA blends will realize the expectation to compact different components and increase the toughness through decreasing the crystalline degree.

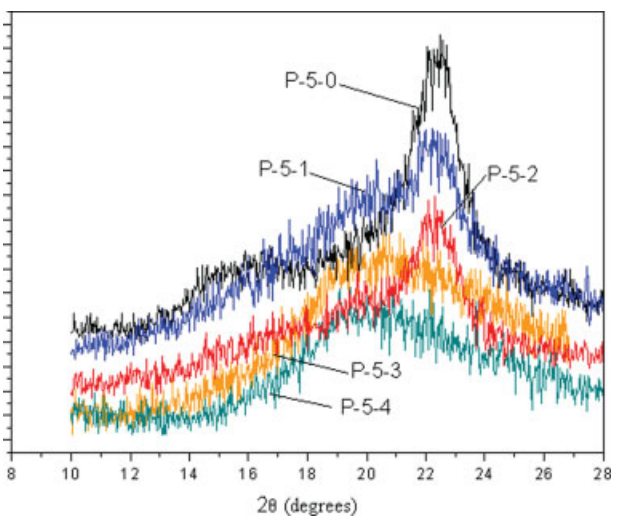

Figure 4 X-ray patterns of the P-5-0, P-5-1, P-5-2, and P-5-3. [Color figure can be viewed in the online issue, which is available at www.interscience.wiley.com.]

To investigate the glass transition behavior is another effective approach to understand the compatibility of SPI and PVA. Although SPI materials have been widely studied, literatures report no consistent result about their T_g. For example, pure SPI without any plasticizers presents a T_g value of about 150°C obtained by dynamic mechanical thermal analysis (DMTA), whereas the T_g of SPI with 25 wt % glycerol decreases to −50°C.[32,33] More recently, Chen and Zhang[34] have investigated the glass transition behaviors and microstructures of SPI by using differential scanning calorimetry (DSC) and small angle X-ray scattering. Interestingly, their results reveal that there are two glass transitions for the SPI/glycerol system. All these researches imply that the microstructure and glass transition of SPI plasticized by glycerol are still uncertain owing to its structural complexity.

Regardless of being an open question, T_g is still a parameter need to be investigated for films fabrication and application in this study. To simplify the complexity of T_g, P-5, P-10, P-15, and P-20 were analyzed to know the difference of their thermal behaviors. The T_g and melting temperature (T_m) thus obtained are shown in Figure 5. T_g is observed to be in the range of from 80 to 115.0°C, whereas T_m

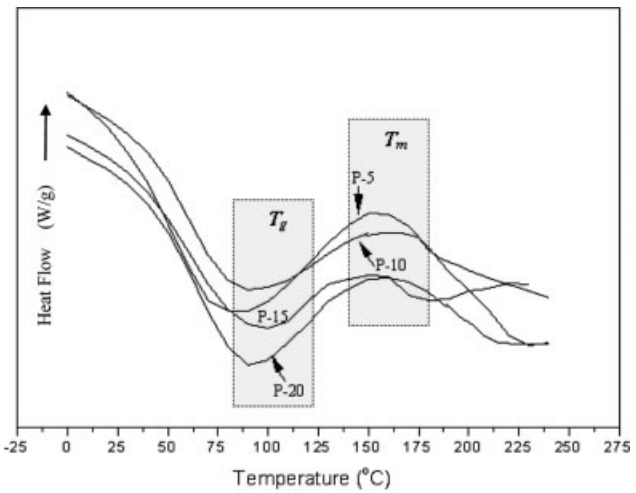

Figure 5 DSC curves of P-5, P-10, P-15, and P-20.

between 130 and 160°C. Each sample has only one T_g higher than that of pure PVA (110.7°C[35]) similar with our previous study.[23] Normally, the single T_g for blend polymers in DSC curve will reflect the good compatibility. These results agree very well with the XRD analysis result discussed earlier. The DSC analysis here indicates that blending process has destroyed both SPI and PVA respective crystalline structures, and the coexistence of PVA may have changed the aggregate structure of pure SPI.

As a kind of protein, SPI has a wide molecular weight ranging from 8 to 600 kDa, which can be fractionated into 2S, 7S, 11S, and 15S according to their sedimentation coefficients. The amino acid composition of 11S and 7S, representing about 70–80% of SPI, determine the major properties of SPI. As a heterogeneous macromolecule, SPI contains 18 kinds of amino acids that can be classified into nonpolar or polar.[36] Originally, the nonpolar amino acids (e.g., glycine, alanine, valine, leucine, isoleucine, methionine, proline, phenylalanine, and tryptophan) constitute nearly 50% of amino acids of SPI. The polar amino acids, ionic (e.g., lysine, histidine, aspartic acid, and glutamic acid) and nonionic (e.g., serine, threonine, tyrosine, asparagine, glutamine, and cysteine), constitute nearly 50% of the amino acids. Therefore, about half of the SPI amino acids could potentially interact with the functional hydroxyl group of the PVA. These functional hydroxyl groups will enhance melting energy and then increase the T_m of blends.

FTIR analysis

The FTIR analysis of films was based on the identification of bands related to functional groups present in SPI and PVA. Figure 6 shows the FTIR spectra of pure SPI powder. The absorption of 3294 cm^{-1} refers

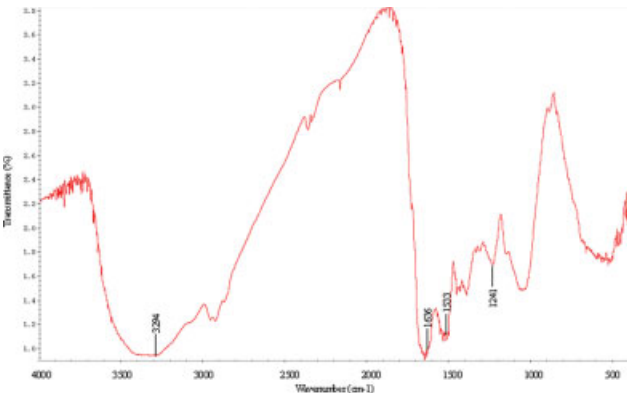

Figure 6 FTIR spectra of pure SPI powder. [Color figure can be viewed in the online issue, which is available at www.interscience.wiley.com.]

to the hydrogen-bond association between protein chains and moisture in protein. There is obvious absorption of —NH— band in the range of 1636–1680 cm^{-1} and 1533–1559 cm^{-1}. These bands accord with the reported soy protein spectrum with an amide I band at 1632 cm^{-1} and amide Π band at 1536 cm^{-1}.[37] In these amino bands, the resulting —NH—CO— bond is called a peptide bond in protein forming primary backbone. The primary polypeptides are further folded into three-dimensional complex protein body for forming secondary, tertiary, and quaternary structure. Therefore, the amino bands can be composed of several overlapping components because of various protein segments with different secondary structures. The absorption band at 1241–1472 cm^{-1} is attributable to the (C)O—O and C—N stretching and N—H bending (amide III) vibrations. The band at ca. 1060 cm^{-1} has been considered as the contribution from different groups such as out-of-plane C—H bending (from aromatic structure) and PO_2 or P—OH stretching from phosphate esters. Figure 7 shows the FTIR spectra of pure PVA powder. The basic structure of PVA molecular is the

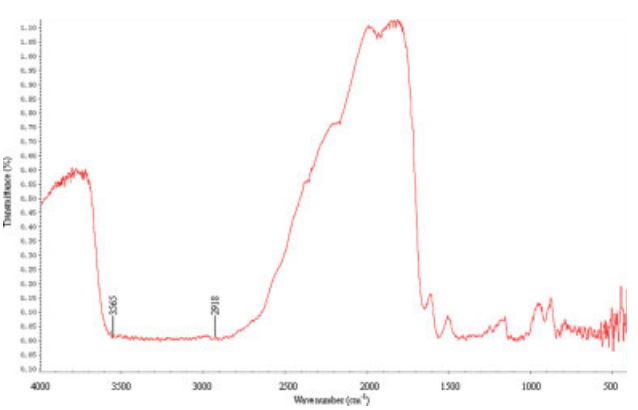

Figure 7 FTIR spectra of pure PVA powder. [Color figure can be viewed in the online issue, which is available at www.interscience.wiley.com.]

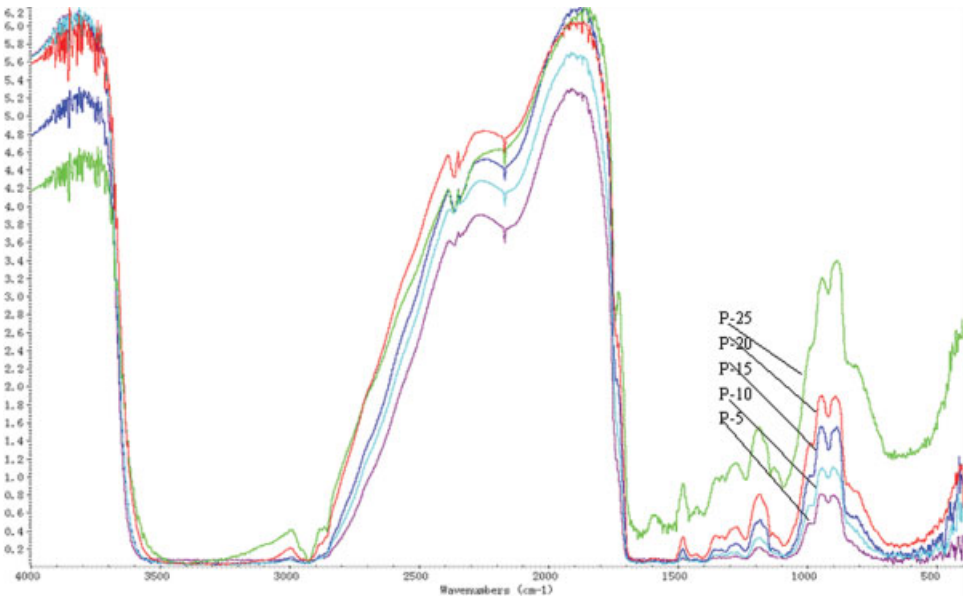

Figure 8 FTIR spectra of P-5, P-10, P-15, P-20, and P-25. [Color figure can be viewed in the online issue, which is available at www.interscience.wiley.com.]

—OH groups on carbon chains. At room temperature, the broad —OH absorption band is observed in the wavenumber range of 2918–3565 cm^{-1}.

The FTIR spectra of P-5, P-10, P-15, P-20, and P-25 are shown in Figure 8. As can be seen in spectra of the blend films, most characteristic absorption bands appear in proportion to the weight ratios of SPI and PVA. The absorption bands at 1600–1400cm^{-1} and 1150–1250 cm^{-1} are attributable to —NH—, C—N stretching, and N—H bending (amide III) vibrations, respectively. A typical characterization of these spectra is the disappearance of the strong hydrogen-bond association appearing both in SPI and PVA spectra, whereas a new absorption band at 2900–3100 cm^{-1} appears. Normally, the absorption band of 2918–3565 cm^{-1} accord to the lapped characteristic band of —OH for moisture in SPI and PVA as mentioned earlier. These band shifts suggest that there may be a specific chemical interaction occurring between SPI and PVA. The new band may be referring to the hydrogen-bond association between protein chains and PVA, which accords with the above analyze by DSC.

Mechanical properties of films

In this study, the mechanical properties of SPI/PVA films depend on the weight contents of PVA without

TABLE I
Effect of PVA Content and Compatibilized by Glycerol on Mechanical Properties of SPI/PVA Films

Samples	σ_y (MPa)	σ_b (MPa)	P.E.Y. (%)	P.E.B. (%)	Strength (MPa)	E (MPa)
P-0-0	41.6	41.2	1.2	1.3	41.6	1227
P-10-0	32.9	28.6	2.4	70.0	34.2	1009
P-20-0	20.6	16.3	3.5	76.1	21.0	300
P-30-0	15.3	8.8	4.3	80.0	10.1	154
P-40-0	8.6	7.9	4.7	80.5	7.4	120
P-0-1	42.2	45.8	2.0	2.7	40.3	1124
P-10-1	43.0	49.2	2.5	20.8	45.8	924
P-20-1	14.3	30.2	4.0	66.1	50.2	250
P-30-1	17.2	16.9	4.5	110.2	52.1	150
P-40-1	9.8	10.5	5.0	125.0	55.1	106
P-0-2	44.8	50.7	2.0	15.4	46.3	1435
P-10-2	39.1	52.8	5.0	50.4	48.4	1112
P-20-2	25.7	18.5	7.1	125.7	55.8	560
P-30-2	19.2	10.9	15.0	139.2	58.5	462
P-40-2	12.8	8.5	50.1	159.0	61.7	321

σ_y is the stress at yield point, σ_b is the stress at break point, P.E.Y. is the percentage elongation at yield point, P.E.B. is the percentage elongation at break point, E is Young's modulus; P-0-0 means SPI/PVA (100/0) without glycerol, P-10-2 means SPI/PVA (100/10) compatibilized by glycerol (2 wt % SPI).

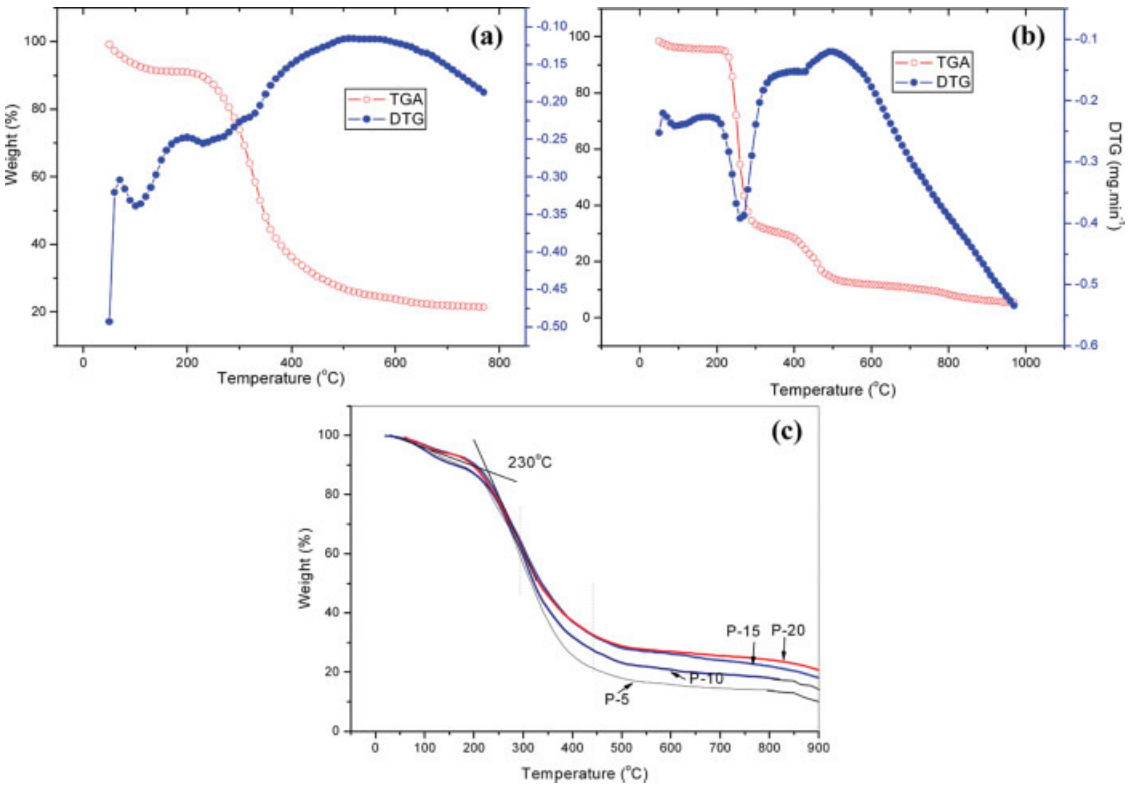

Figure 9 The thermogravimetric (TGA) curves of (a) SPI powder, (b) PVA powder, and (c) SPI/PVA samples of P-5, P-10, P-15, and P-20. [Color figure can be viewed in the online issue, which is available at www.interscience.wiley.com.]

considering its hydrolysis degrees. Concretely, data of mechanical properties are shown in Table I. Yield point (σ_y), break point (σ_b), percentage elongation at yield point (P.E.Y.), percentage elongations at break point (P.E.B.) were measured automatically and Young's modules (E) was calculated from the tensile stress–strain plots by the computer software.

The following results can be concluded from these data: (1) For SPI/PVA samples without glycerol, we can find that both values of σ_y and σ_b decreased with the increasing of PVA content from 41.6 to 8.6 Mpa and from 41.2 to 7.9 Mpa, respectively. (2) Comparing to the above SPI/PVA samples without glycerol, the values of σ_y and σ_b for each sample compatibilized by glycerol have been improved. For example, for P-10 and P-10-1, σ_y and σ_b have increased from 32.9 to 43.0 Mpa and from 28.6 to 49.2 Mpa. (3) With the increasing of glycerol weight (from 1.0 to 2.0 wt % of SPI) in films, both of σ_y and σ_b are increased for each sample. (4) For each sample, data of P.E.Y. and P.E.B. are all enlarged after adding glycerol. For example, P.E.Y. for P-10, P-10-1, and P-10-2 are 2.4, 2.5, and 5.0 Mpa, and P.E.B. for P-10, P-10-1, and P-10-2 are 70, 20.8, and 50.4 Mpa. (5) Moreover, data of Young's modules from P-0 to P-40 have been decreased with the compatibility of glycerol, which indicate that the blend becomes softer with the plasticization of glycerol.

These enhanced mechanical properties can attribute to the long-chain PVA molecules, which contain many —OH groups forming strong intra- and intermolecules interactions with protein molecules. These interactions may include hydrogen-bonding, dipole–dipole, and charge effects. In addition, blending long molecules in SPI could bring about molecular entanglements, which in turn will improve the mechanical properties of SPI. On the other hand, the strength, toughness, and Young's modulus values decreased with decreasing crystallinity in SPI/PVA blend polymer.

Thermal stability of films

In Figure 9, the thermogravimetric (TGA) curves of SPI powder [Fig. 9(a)], PVA powder [Fig. 9(b)], and SPI/PVA blends [Fig. 9(c)] are shown. As a nature material, SPI has a lower decomposing temperature at about 110°C. In the beginning 100°C, about 10% weight had lost owing to the moisture. Commonly, PVA decomposing temperature is in the range of 200–220°C. In this test, PVA powder has a decomposing temperature at about 220°C. Samples of P-5, P-10, P-15, and P-20 decomposed at nearly same temperature of 230°C. Accordingly, 15% moisture weight lost in the temperature range of 0–150°C. However, different decomposing ratios appear for

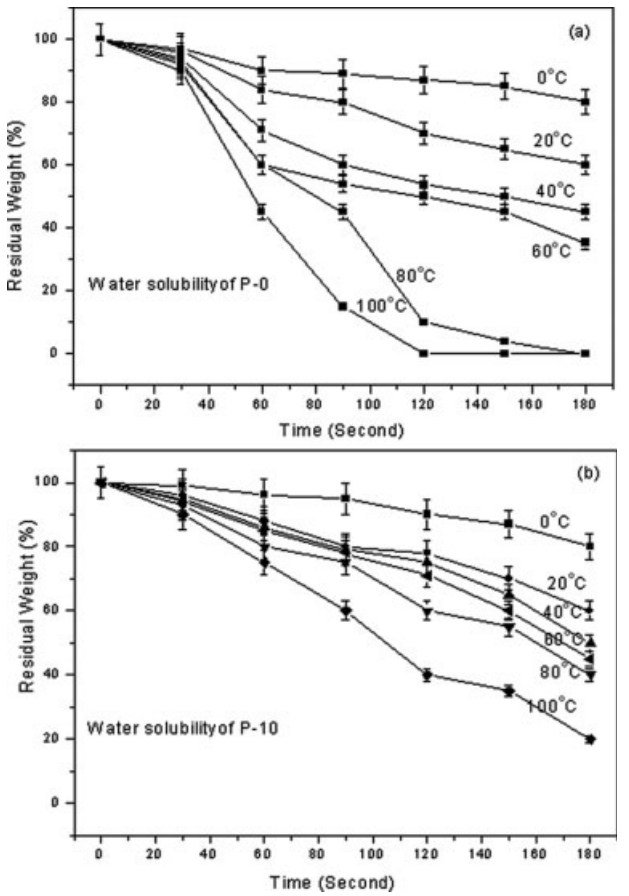

Figure 10 The data of solubility in water at various temperatures for (a) P-0 and (b) P-10.

these samples during the losing-weight process from 60 to 20 wt %. Obviously, P-5 has the maximal slope of weight-temperature line in this part. With the increasing of content of PVA in SPI/PVA blends, the values of slope of weight-temperature line were reduced. We can conclude from these curves straightway that blend films have higher thermal stability than pure SPI powder. In addition, the TGA curves of P-5, P-10, P-15, and P-20 have a decomposing temperature at about 230°C higher than both of SPI and PVA. A beginning temperature may be 250°C, following various decomposing ratios with different PVA contents in films. With the increasing weight ratios of PVA, the decomposing speeds decreased attributing the higher thermal stability.

Testing solubility in water is another method to detect the thermal stability for soluble films. PVA is water-soluble and SPI is water-sensitive, which results in the water-sensitivity of their blends. Therefore, any measures for reducing water-sensitivity of the blend films is very meaningful for the applications of these films. Moreover, as a "green" polymeric material, SPI/PVA needs a relatively good stability in water for a relative longer service time in application. Originally, the water solubility of polymers is determined by their molecular structures including crystallinity or crosslinkage. Therefore, structure and thermal stability information may be achieved through the dissolution tests. The solubility data of the films in water at various temperatures are shown in Figure 10. Compared the residual weight of P-0 and P-10, following results can be achieved from these data: (1) dissolution speed was accelerated with the increasing of temperature for each sample, (2) pure SPI film entirely dissolved in 180 s and P-10 has a lower dissolution speed than P-0, (3) interestingly, for P-10 under the condition of 100°C in water at time of 180 s, there is still about 20% residual weight in solid state. Normally, 10% PVA in P-10 nearly did not lost in just 180 s in at 100°C. Therefore, the other 10% residual weight only was SPI material. Based the above analyses, we know that the SPI and PVA certainly formed somewhat internal structure. The stronger interactions between SPI and PVA resist the water molecular permeating through films.

CONCLUSIONS

A variety of SPI/PVA blend films were successfully prepared by a solution-casting method. Properties of compatibility, mechanical properties, and thermal stability were analyzed using measures of tension test, SEM, XRD, FTIR, DSC, and TGA. These films are smooth with rolling condition and good transparence. Mechanical properties indicate that SPI/PVA films have high tensile strength (σ_b) and percentage elongation at break point (P.E.B.) than pure SPI films. Young's modules has been decreased with the compatibility of glycerol, which implies that the blend becomes soft with the plasticization of glycerol. XRD and DSC tests show that the SPI/PVA films have good compatibility, and the presence of glycerol has reduced the crystallinity of PVA/SPI blends.

The authors gratefully acknowledge the help of Harbin High-Tech Soybean Food Co., Ltd.

References

1. Zhou, Z.; Zheng, H.; Wei, M.; Huang, J.; Chen, Y. J Appl Polym Sci 2008, 107, 3267.
2. Zhong, Z. K.; Sun, X. Z. S.; Wang, D. H. J Appl Polym Sci 2007, 103, 2261.
3. Rhim, J. W. Food Sci Biotechnol 2007, 16, 62.
4. Mohareb, E.; Mittal, G. S. Packag Technol Sci 2007, 20, 1.
5. Patel, J. D.; Ebert, M.; Ward, R.; Anderson, J. M. J Biomed Mater Res A 2007, 80, 742.
6. Nanda, P. K.; Rao, K. K.; Nayak, P. L. J Appl Polym Sci 2007, 103, 3134.
7. Cho, S. Y.; Park, J. W.; Batt, H. P.; Thomas, R. L. LWT-Food Sci Technol 2007, 40, 418.
8. Rhim, J. W.; Lee, J. H.; Hong, S. I. LWT-Food Sci Technol 2006, 39, 806.

9. Ralston, B. E.; Osswald, T. A. Plast Eng 2008, 64, 36.
10. Hernandez-Izquierdo, V. M.; Krochta, J. M. J Food Sci 2008, 73, R30.
11. Kurose, T.; Urman, K.; Otaigbe, J. U.; Lochhead, R. Y.; Thames, S. F. Polym Eng Sci 2007, 47, 374.
12. Hua, Z.; Ziyan, Z.; Yun, C.; Jin, H.; Fuliang, X. J Appl Polym Sci 2007, 106, 1034.
13. Shiyi, O.; Yong, W.; Shuze, T.; Caihuan, H.; Jackson, M. G. J Food Eng 2005, 70, 205.
14. Liu, D. G.; Zhang, L. N. Macromol Mater Eng 2006, 291, 820.
15. Dicharry, R. M.; Ye, P.; Saha, G.; Waxman, E.; Asandei, A. D.; Parnas, R. S. Biomacromolecules 2006, 7, 2837.
16. Chen, P.; Zhang, L. N.; Peng, S. P.; Liao, B. J Appl Polym Sci 2006, 101, 334.
17. Silva, S. S.; Santos, M. I.; Coutinho, O. P.; Mano, J. F.; Reis, R. L. J Mater Sci: Mater Med 2005, 16, 575.
18. Kumar, R.; Liu, D.; Zhang, L. J Biobased Mater Bioenergy 2008, 2, 1.
19. Cakmakli, B.; Hazer, B.; Acikgoz, S.; Can, M.; Comert, F. B. J Appl Polym Sci 2007, 105, 3448.
20. Swain, S. N.; Biswal, S. M.; Nanda, P. K.; Nayak, P. L. J Polym Environ 2004, 12, 35.
21. Huang, J.; Zhang, L.; Wang, X. H. J Appl Polym Sci 2003, 89, 1685.
22. Zheng, H.; Tan, Z. A.; Zhan, Y. R.; Huang, J. J Appl Polym Sci 2003, 90, 3676.
23. Su, J. F.; Huang, Z.; Liu, K.; Fu, L. L.; Liu, H. R. Polym Bull 2007, 58, 913.
24. Lodha, P. Ind Crops Prod 2005, 21, 49.
25. Martelli, S. M.; Moore, G. R. P.; Laurindo, J. B. J Polym Environ 2006, 14, 215.
26. Bourriot, S.; Garnier, C.; Doublier, J. L. Carbohydr Polym 1999, 40, 145.
27. Cho, S. Y.; Rhee, C. LWT-Food Sci Technol 2002, 35, 151.
28. Chiellini, E.; Cinelli, P.; Corti, A.; Kenawy, E. R. Polym Degrad Stab 2001, 73, 549.
29. Kaczmarek, H.; Podgórski, A. J Photochem Photobiol A 2007, 191, 209.
30. Yakimets, I.; Wellner, N.; Smith, A. C.; Wilson, R. H.; Farhat, I.; Mitchell, J. Polymer 2005, 46, 12577.
31. Xiao, C. M.; Gao, Y. K. J Appl Polym Sci 2008, 107, 1568.
32. Zhang, J.; Mungara, P.; Jane, J. Polymer 2001, 42, 2569.
33. Sue, H. J.; Wang, S.; Jane, J. L. Polymer 1997, 38, 5035.
34. Chen, P.; Zhang, L. N. Macromol Biosci 2005, 5, 237.
35. Mendieta-Taboada, O.; Sobralb, P. J. A.; Carvalhob, R. A.; Habitanteb, A. M. B. Q. Food Hydrocolloid 2008, 22, 1485.
36. Schmidt, V.; Soldi, V. Polym Degrad Stab 2006, 91, 3124.
37. Barreto, P. L. M.; Pires, A. T. N.; Soldi, V. Polym Degrad Stab 2003, 79, 147.